Environmental Science Processes & Impacts

PAPER

View Article Online
View Journal



Cite this: DOI: 10.1039/d2em00349j

# Non-targeted identification and semi-quantitation of emerging per- and polyfluoroalkyl substances (PFAS) in US rainwater †

Yubin Kim,[a] Kyndal A. Pike,‡[ab] Rebekah Gray,[a] Jameson W. Sprankle,[ac] Jennifer A. Faust[a] and Paul L. Edmiston[*a]

High-resolution mass spectrometry was used to screen for emerging per- and polyfluorinated alkyl substances (PFAS) in precipitation samples collected in summer 2019 at seven sites in the United States. We previously quantified the concentration of ten PFAS in the rainwater samples using the method of isotopic dilution (Pike *et al.*, 2021). Nine of these targeted analytes belonged to the U.S. Environmental Protection Agency Regional Screening Level list, herein referred to as EPA-monitored analytes. In this new work, we identify emerging PFAS compounds by liquid chromatography quadrupole time-of-flight mass spectrometry. Several emerging PFAS were detected across all samples, with the most prevalent compounds being C3–C8 hydrogen-substituted perfluorocarboxylic acids (H-PFCAs) and fluorotelomer carboxylic acids (FTCAs). Concentrations of emerging PFAS were in the 10–1000 ng $L^{-1}$ range (approximately 1–2 orders of magnitude greater than EPA-monitored PFAS) at all sites except Wooster, OH, where concentrations were even higher, with a maximum estimated $\Sigma_{PFAS}$ of 16 400 ng $L^{-1}$. The elevated levels of emerging PFAS in the Wooster samples were predominantly even and odd chain-length H-PFCAs and FTCAs comprised of complex mixtures of branched isomers. This unique composition did not match any known manufactured PFAS formulation reported to date, but it could represent thermally transformed by-products emitted by a local point source. Overall, the results indicate that PFAS outside of the standard analyte lists make up a significant and previously unappreciated fraction of contaminants in rainwater collected within the central U.S.—and potentially world-wide—especially in proximity to localized point sources.

Received 23rd August 2022
Accepted 29th October 2022

DOI: 10.1039/d2em00349j

rsc.li/espi



### Environmental significance

PFAS, or per- and polyfluorinated alkyl substances, are ubiquitous chemicals that are both toxic to humans and long-lived in the environment. Typically only a handful of PFAS are routinely monitored in the environment, and only four are regulated in drinking water across the United States. Here we used high-resolution mass spectrometry to identify over 20 emerging PFAS in rainwater samples from seven U.S. sites. (Note: emerging PFAS is defined as compounds that do not appear as EPA Method 533 and/or 537.1 analytes). The most prevalent PFAS were highly branched polyfluorinated carboxylic acids. Wet deposition of these compounds from the atmosphere could represent an important yet ignored source of PFAS contamination. Results from our regional sampling network suggest that local point sources exert a significant influence on the isomeric profiles and deposition fluxes of PFAS in precipitation.

## Introduction

PFAS, or per- and polyfluoroalkyl substances, are anthropogenic chemicals with a wide variety of uses, ranging from manufacturing to consumer products to firefighting.[1] PFAS are highly persistent in the environment, and they can enter the atmosphere through direct emissions or through degradation of precursors.[2,3] Once in the atmosphere, PFAS and their precursors can undergo long-range transport in the gas phase or in the particle phase and return to Earth through wet and dry deposition.[4–9] Accordingly, PFAS have been detected at remote locations such as the Arctic,[5,10–13] the Antarctic,[14,15] and open oceans[16] that are far from any possible point sources. Transport and deposition of PFAS is of concern because of the negative impacts of PFAS on ecosystems and human health.[17–21]

Here we focus on atmospheric transport of emerging PFAS through precipitation. PFAS removal by wet deposition depends

[a]Department of Chemistry, College of Wooster, Wooster, OH, USA. E-mail: pedmiston@wooster.edu

[b]Department of Mathematical & Computational Sciences, College of Wooster, Wooster, OH, USA

[c]Department of Earth Sciences, College of Wooster, Wooster, OH, USA

† Electronic supplementary information (ESI) available. See DOI: https://doi.org/10.1039/d2em00349j

‡ Current affiliation: Department of Chemistry, University of Wisconsin–Madison, Madison, WI, USA.

on rain–air partition coefficients from the gas phase and from the particle phase.[15,22] PFAS have been detected in precipitation from urban, rural, and remote sites around the world.[9] Most studies have focused on deposition of perfluorinated carboxylic acids (PFCAs) and perfluorinated sulfonic acids (PFSAs) because historically these classes were in the most widespread use, particularly the C8 species PFOA (perfluorooctanoic acid) and PFOS (perfluorooctane sulfonic acid).[15,22–30] Other species previously analyzed in wet deposition include perfluoroalkane sulfinic acids,[31] perfluorinated ether carboxylic acids (PFECAs),[32,33] perfluoroalkane sulfonamides,[16,31,34,35] perfluoroalkane sulfonamido ethanols,[36] perfluoroalkyl sulfonamido acetic acids,[31,35] fluorotelomer carboxylic acids (FTCAs),[31,35,37,38] fluorotelomer sulfonic acids,[39] fluorotelomer unsaturated carboxylic acids (FTUCAs),[16,31,34,35,37–39] and chlorinated PFAS.[39] The acronyms for PFAS classes are summarized in Table S1.† In this work, we use FTCAs to describe PFCAs with two F atom to H atom substitutions regardless of the position of the H or whether the chain length is even or odd, and we use H-PFCAs (hydrogen-substituted PFCAs) for a single F atom to H atom substitution, in keeping with the notation in the FluoroMatch library.[40]

PFAS are a diverse group of chemical compounds, encompassing thousands of structures, and rapidly changing regulations are driving innovation among manufacturers.[41,42] For example, as restrictions on the use of PFOA and PFOS spread, shorter-chain species and species of other functional classes, such as the C6 ether acid hexafluoropropylene oxide dimer acid (HFPO-DA, trade name GenX) have become more prevalent.[43–45] Based on total oxidizable precursor assays, only a fraction of PFAS present in most environmental samples have been detected by targeted approaches.[39,46] With advances in high-resolution mass spectrometry (HR-MS), non-targeted analysis (NTA) has become a powerful tool for solving the mystery of the unknown fraction.[44,47–49] NTA allows for the identification of unknown compounds without any *a priori* assumptions about the sample.[50,51] Formulae can be determined from accurate mass measurements and isotopic distributions, and structures can be predicted from MS/MS fragmentation patterns through comparison to experimental measurements or to *in silico* calculations. Closely related to NTA is suspect screening, in which high-resolution mass spectra are screened against extensive libraries. Among the many applications of HR-MS for PFAS analysis in aqueous media, suspect screening and NTA have been used to identify emerging PFAS in surface waters,[52–56] industrial wastewater,[57,58] municipal wastewater treatment plants,[59,60] and on particulate matter.[61,62]

Comprehensive measurements by HR-MS facilitate source tracking of PFAS.[63,64] The isomeric profile of linear *versus* branched species acts as a sort of fingerprint for the compounds' origins.[65] The manufacturing process of electrochemical fluorination (ECF) produces a mixture of linear and branched products: 70–80% linear for PFOS, 80–85% linear for PFOA, and ~95% linear for PFHxS (perfluorohexane sulfonic acid, C6), for example.[66] Telomerization, in contrast, preserves the stereochemistry of the starting material (usually linear). Targeted mass spectrometry with selective reaction monitoring can inaccurately measure the isomeric PFAS profile if the chosen transitions do not capture all isomers and/or chromatographic separation is insufficient. Determining whether the isomeric profile matches ECF is further complicated because stereochemistry affects reactivity, acidity, water solubility, and partitioning.[65–70] Measuring the isomeric profile of PFAS in a single compartment of the environment is often insufficient to definitively assign sources.[27,71–75] Nevertheless, isomeric profiles have been used to determine that fluorotelomer alcohol (FTOH) degradation was the major source of PFAS deposition to alpine lakes[76] and that a Norwegian lake was contaminated with PFAS from a paper factory and not from a fire station.[75] For atmospheric samples, branched PFAS isomers have been quantified in precipitation from semirural and urban Canada;[27] in precipitation from the urban centers of Beijing, Wuhan, and Stockholm;[24] in precipitation from islands off the coasts of Sweden and Portugal;[24] and in particulate matter from urban centers in China.[77,78] To the best of our knowledge, there have been no studies of PFAS isomers in wet or dry deposition samples in the United States.

Here we report the first applications of suspect screening and NTA to identify and semi-quantitate PFAS in wet deposition. This work expands on our earlier targeted measurements of the C2 and C4–C10 PFCAs, PFOS, and HFPO-DA in rainwater at six sites in the Ohio/Indiana region of the central United States, with a reference site at approximately the same latitude in Wyoming.[32] The sampling network included a mix of rural, suburban, and semi-urban locations with no known point sources near any of the collection sites. PFAS, including HFPO-DA, were present in all samples from all sites in summer 2019. The concentrations at the Wooster, Ohio site were significantly elevated compared to the other locations ($p < 0.05$). With new HR-MS measurements for suspect screening and NTA, we seek to answer the question: What are we missing with the narrow, targeted approach?

Our goals here are: (1) to identify and semi-quantitate emerging PFAS in precipitation samples from the central United States, and (2) to assess sources and spatial trends of PFAS through regional atmospheric transport. First, we used liquid chromatography quadrupole time-of-flight mass spectrometry (LC-QTOF-MS) to analyze rainwater samples in MS-only mode to screen mass-to-charge ratios against accurate mass lists from FluoroMatch[40] and NIST.[79] We then built a list of preferred ions for data-dependent acquisition of MS/MS spectra, and we screened the resulting mass spectra against the FluoroMatch library. We supplemented suspect screening with NTA using a $CF_2$ Kendrick mass defect analysis for homologous series of FTCAs and H-substituted PFCAs,[58,80] as well as cross-checks against characteristic fragmentation and neutral loss patterns for PFAS.[55,59,81] We semi-quantitated all identified PFAS with isotopically labelled surrogates, and we conducted statistical analyses with Kruskal–Wallis tests, principal component analysis (PCA), and Kendall's tau correlations. Finally, we used HYSPLIT[82,83] to model air mass back trajectories prior to precipitation events.

 

# Methods

## Reagents

Isotopically labelled PFAS standards were obtained from Wellington (Guelph, ON, Canada), as was the mixture of FTCA standards (2-perfluorohexyl ethanoic acid, 2-perfluorooctyl ethanoic acid, and 2-perfluorodecyl ethanoic acid). Perfluoropropionic acid and ammonium acetate (LC-MS grade) were obtained from Sigma Aldrich (St. Louis, MO, USA). Solvents included LC-MS grade methanol (EMD Millipore) and Nanopure water (18.2 MΩ cm).

## Sampling

Fig. S1† shows a map of the seven collection sites: Ashland, OH (semiurban; 40.9°N, 82.3°W); Rockford, OH (rural; 40.7°N, 84.6°W); Shaker Heights, OH (suburban; 41.5°N, 81.6°W); Whitestown, IN (suburban; 40.0°N, 86.4°W); Willoughby, OH (suburban; 41.6°N, 81.4°W); Wooster, OH (industrial; 40.8°N, 81.9°W); and Jackson Hole, WY (reference; 43.5°N, 110.8°W). The Wyoming site was selected because it is located at approximately the same latitude at the Indiana/Ohio sites but at a distance of ~2500 km. As described in Pike *et al.*,[32] rainwater was collected during precipitation events between May and August of 2019. Samples were collected in high-density polyethylene (HDPE) tubs and stored in HDPE bottles at 4 °C. At the Wooster site, a HDPE funnel and carboy were used in place of the tub. Site blanks to check for contributions from dry deposition were collected at the beginning and end of the campaign. On a day without rain, 1 L of nanopure water was placed in the tub or carboy and allowed to remain exposed to the atmosphere for 24–48 hours. A ride-along blank was also prepared for the Whitestown site by shipping a 1 L bottle of nanopure water along with the sample bottles. Sample analysis was conducted in Wooster, OH. Table S2 in the ESI† lists the number of samples and blanks from each site.

## Sample preparation

Full details of the sample preparation procedure are given elsewhere.[31,32] Briefly, samples were spiked with 5.6 ng of each of the following isotopically labelled standards: perfluoro-*n*-[1,2,3,4-$^{13}$C4]butanoic acid (M4PFBA); perfluoro-*n*-[3,4,5-$^{13}$C3]pentanoic acid (M3PFPeA); perfluoro-*n*-[1,2-$^{13}$C2]hexanoic acid (M2PFHxA); perfluoro-*n*-[1,2,3,4-$^{13}$C4]heptanoic acid (M4PFHpA); perfluoro-*n*-[1,2,3,4-$^{13}$C4]octanoic acid (M4PFOA); perfluoro-*n*-[1,2,3,4,5-$^{13}$C5]nonanoic acid (M5PFNA); perfluoro-*n*-[1,2-$^{13}$C2]decanoic acid (MPFDA); sodium perfluoro-1-[2,3,4-$^{13}$C3]butanesulfonate (M3PFBS); sodium perfluoro-1-hexane[$^{18}$O2] sulfonate (MPFHxS); sodium perfluoro-1-[1,2,3,4-$^{13}$C4]octanesulfonate (M4PFOS); and 2,3,3,3-tetrafluoro-2-(1,1,2,2,3,3,3-heptafluoropropoxy)-$^{13}$C3-propanoic acid (M3HFPO-DA). Each sample, typically between 500 mL to 1 L, was concentrated by solid-phase extraction (SPE) with Oasis WAX cartridges (250 mg, Waters). SPE cartridges were conditioned with 4 mL of methanol + 0.1% ammonia, 4 mL of methanol, and 5 mL of nanopure water. The sample was applied, and cartridges were rinsed with 5 mL of nanopure water. A first elution step was conducted with 4 mL of methanol to collect neutral PFAS, which were not analyzed here. A second elution step was conducted with 4 mL of methanol + 0.1% ammonia to collect the eluate analyzed in this work. Eluates were evaporated to dryness using a homebuilt, Teflon-free nitrogen evaporator, and samples were reconstituted in 250 μL of methanol. A pooled sample was prepared by combining 10 μL aliquots of all the reconstituted sample extracts including blanks.

## Instrumentation

Samples were analyzed with an Agilent 1260 Infinity II liquid chromatograph and Agilent 6545 quadrupole time-of-flight mass spectrometer. A C18 column was used for the chromatographic separation, and negative electrospray was used for ionization. Data were first collected in MS-only mode, and all samples were subsequently re-analyzed through data-dependent MS/MS acquisition with a preferred ions list. Full method details for chromatography and mass spectrometry are provided in Table S3.†

## Data analysis

The Agilent MassHunter 10.0 software suite and the open-source software MS-DIAL (version 4.60)[84] were used for data processing. The FluoroMatch PFAS library was used for suspect screening.[40] MS-DIAL parameters are summarized in Table S4.† Strategies for feature reduction, suspect screening, and non-targeted analysis are discussed in the Results section.

## Semiquantitation

Concentrations of emerging PFAS were estimated by scaling the peak area of the analyte against the peak area of the isotopically labelled surrogate closest in retention time.[85] Because surrogates were added prior to solid-phase extraction, their concentrations in the samples are known exactly.[32] This semi-quantitative calculation introduces appreciable uncertainty when the analyte and the surrogate are not structurally similar and their relative extraction efficiencies, ionization efficiencies, *etc.* are unknown. Nevertheless, concentration ratios from one sample to another remain meaningful with this scaling method since the samples are similar in composition.

Next, concentrations (mass per volume) were converted to estimated deposition fluxes (mass per unit area) using precipitation amounts from the nearest National Weather Service station.[86] The deposition flux $F$ in ng m$^{-2}$ is given by:

$$F = 1000 \times C \times d \quad (1)$$

where $C$ is the concentration in ng L$^{-1}$, $d$ is the rainfall amount in meters, and 1000 is a conversion factor between m$^3$ and L. Calculating flux rather than concentration is necessary to account for washout and scavenging of PFAS at the start of a precipitation event.[16] Further discussion of the uncertainties in deposition flux can be found in Pike *et al.*[32]

### QA/QC

The Non-Targeted Analysis (NTA) Study Reporting Tool (SRT) was used in designing QA/QC measures and preparing this manuscript.[87,88] Isotopically labeled PFAS surrogates were added to precipitation samples prior to solid-phase extraction, as described previously[32] (see Table S5† and Sample Preparation section for list of surrogates). Recoveries and analysis of blanks were outlined previously and shown to be acceptable; results are summarized in Table S6 and S7.†[32] All precipitation extracts were analyzed by LC-QTOF in random order on a contiguous worklist. Prior to measurement, a pooled sample containing 10 μL of each precipitation extract sample (including site blanks) was prepared. The pooled sample, an instrument blank, and a standard mixture containing 5 ng $mL^{-1}$ of each PFAS (Table S8†) were measured after every eighth sample in the worklist. The standard deviation of the retention time and relative standard deviation of peak areas are listed in Table S8† for the standard and Table S9† for the pooled sample. Standards of perfluoropropionic acid and fluorotelomer carboxylic acids were analyzed separately using the same method as samples. Upon re-analysis using data-dependent MS/MS acquisition, the same worklist (with inclusion of instrument blanks, pooled sample replicates, and instrument performance check standards) was used. Inclusion of a feature as a suspect PFAS required the peak area to be statistically higher than peak areas found in instrument and site blanks. Concentrations in the site blanks were not subtracted from concentrations in the samples. Instead, compounds that did not have concentrations significantly higher in the samples than in the blanks (by a one-sided *t*-test, $p < 0.05$) were removed from further analysis.

### Statistics

Analyses and visualization were carried out using RStudio (version 4.1.2).[89] Non-parametric tests were selected due to the data not following a normal distribution. Statistical analyses performed include Kruskal–Wallis tests, pairwise Wilcoxon Rank Sum post-hoc tests, Kendall's tau correlations, and principal component analysis (PCA). For all statistical tests, values below the detection limit were replaced with a value of zero. Results with a *p*-value less than 0.05 were considered significant.

### HYSPLIT

The Hybrid Single-Particle Lagrangian Integrated Trajectory model (HYSPLIT version 5) was used to calculate air mass back trajectories for each rain event.[83] Meteorological data came from the National Centers for Environmental Prediction/National Center for Atmospheric Research (NCEP/NCAR) Reanalysis Project at 2.5° × 2.5° spatial resolution and 6 hours temporal resolution.[90] From the origin at the collection site, trajectories at 500, 1000, and 3000 m above ground level were traced backwards six days with a new trajectory added every four hours.

## Results and discussion

### PFAS identification

All precipitation standards and a pooled sample were measured by LC-QTOF in MS-only mode. The data as a collective were peak-aligned and processed with MS-DIAL (version 4.60)[84] using a FluoroMatch library (version 2.431)[40,91] to find molecular features that may be attributed to PFAS. The initial screen of the MS-only data identified 10 594 potential PFAS features, the majority of which had negative mass defects. High-quality features were identified by selecting those with the following five criteria filtered in the order listed: (i) signal-to-noise (S/N) ratio > 200, (ii) quality scores > 90%, (iii) peak heights > 15 000 in the pooled sample, (iv) formulae that contained only F as a halogen, (v) and a putative identification determined to be reasonable based on retention time compared to standards (within 0.2 min). Relatively high data quality thresholds were applied in order to provide certainty to the identifications since there are few studies of emerging PFAS in precipitation. Application of the criteria resulted in 96 features. The 96 high-quality features were then added as preferred ions in a MS/MS re-analysis of the samples by LC-QTOF in the Auto-MS/MS mode of Agilent MassHunter Acquisition 10.0 software. Data were then analyzed using the FluoroMatch MS/MS library *via* MS-DIAL, resulting in 979 features. The number was further reduced to 74 high-quality features based on S/N and retention time criteria. The 74 high-quality features were further assessed by verifying fragment ion matches found in MS/MS library spectra. Since most of the 74 compounds differed only by chain length, Kendrick mass defect plots were used to validate the assignments (Fig. S2†). Many of the 74 compounds were H-substituted perfluorocarboxylates of various chain lengths, eluted stepwise chromatographically within the homologous series (Fig. S3†). Application of all the criteria above resulted in the identification of 24 emerging PFAS compounds with confidence levels of **3a** or above according to the scale defined by Charbonnet *et al.*[92] See Table 1 for the list of emerging PFAS and Appendix A of the ESI† for full data. As a final check, the MS-only data set was re-screened using the NIST PFAS suspect list[79] and Agilent MassHunter Qualitative Analysis (version 10.0). The NIST suspect screening in MassHunter identified a total of 3935 features, including the 74 high-quality features determined *via* the analysis through MS-DIAL using the FluoroMatch library. It is noted that the stringency of the data analysis likely excluded low-abundance features. Further searches for additional emerging PFAS can be done in the future, and data are available upon request.

Reference standards were commercially available for compounds 2, perfluoropropionic acid (PFPrA); **11**, 2-perfluorohexyl ethanoic acid (6 : 2 FTCA); **17**, 2-perfluorooctyl ethanoic acid (8 : 2 FTCA); and **21**, 2-perfluorodecyl ethanoic acid (10 : 2 FTCA), according to the numbering scheme in Table 1. The standards were analyzed with the same LC-QTOF method used for the samples in both MS-only and MS/MS modes. Retention times matched the presumed linear version of the features in the samples, allowing a level 1 confidence according

 

Table 1 Emerging PFAS analytes identified by non-targeted analysis, mass spectral data, and confidence levels

| Compound | Structure (linear isomer) | Formula | RT | Ref Mass | *m/z* | Δppm | MS/MS 1 | MS/MS 2 | MS/MS 3 | Surrogate | Confidence |
|---|---|---|---|---|---|---|---|---|---|---|---|
| (**1**) 2 : 2 FT carboxylic acid | 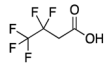 | $C_4H_3F_5O_2$ | 3.21 | 176.9981 | 176.9980 | 0.08 | 92.9950 | | | MPFPeA | **2a** |
| (**2**) Perfluoropropionic acid |  | $C_3HF_5O_2$ | 3.55 | 162.9824 | 162.9828 | 0.40 | 118.9933 | | | MPFPeA | **1a** |
| (**3**) 3 : 2 FT carboxylic acid ($n = 3$) | 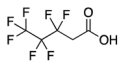 | $C_5H_3F_7O_2$ | 4.97 | 226.9949 | 226.9954 | 0.56 | 92.9958 | 142.9930 | | MPFPeA | **2b** |
| (**4**) PFCA-perfluoroalkyl-H-substituted-1DB ($n = 2$) | 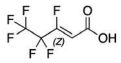 | $C_5H_2F_6O_2$ | 5.89 | 206.9886 | 206.9880 | 0.57 | 92.9958 | 142.9940 | | MPFPeA | **2a** |
| (**5**) Perfluoropropane sulfonate | 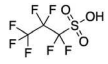 | $C_3HF_7O_3S$ | 6.83 | 248.9462 | 248.9460 | 0.21 | 79.9576 | 98.9561 | | MPFBS | **2b** |
| (**6**) H-substituted perfluoroalkyl dioic acid ($n = 7$) |  | $C_{10}H_3F_{15}O_4$ | 6.83 | 470.9719 | 470.9730 | 1.16 | 192.9895 | 292.9837 | 342.9815 | MPFDA | **2a** |
| (**7**) Unsaturated-ether-PFCA ($n = 2$) | 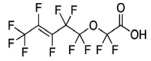 | $C_7HF_{11}O_3$ | 7.47 | 340.9677 | 340.9678 | 0.06 | 118.9935 | | | MPFHpA | **2c** |
| (**8**) H-substituted perfluoroalkyl dioic acid($n = 8$) |  | $C_{11}H_3F_{17}O_4$ | 9.14 | 520.9687 | 520.9692 | 0.49 | 242.9871 | | | MPFDA | **2b** |
| (**9**) OPFC-perfluoroalkyl sulfate ($n = 4$) |  | $C_8H_{10}F_8O_4S$ | 10.53 | 353.0099 | 353.0032 | 6.69 | 204.9903 | | | MPFOS | **3a** |
| (**10**) H-substituted-unsaturated ether-PFCA ($n = 7$) |  | $C_{12}H_4F_{18}O_3$ | 11.42 | 536.9800 | 536.9777 | 2.32 | 192.9889 | 242.9871 | 292.9826 | MPFDA | **3a** |
| (**11**) 6 : 2 FT carboxylic acid ($n = 6$) |  | $C_8H_3F_{13}O_2$ | 11.66 | 376.9853 | 376.9846 | 0.67 | 92.9959 | 242.9886 | 292.9831 | MPFOA | **1a** |
| (**12**) H-substituted-PFCA ($n = 5$) |  | $C_7H_2F_{12}O_2$ | 11.98 | 344.9790 | 344.9790 | 0.00 | 118.9902 | 280.9828 | | MPFHpA | **2a** |
| (**13**) 7 : 2 FT carboxylic acid ($n = 7$) |  | $C_9H_3F_{15}O_2$ | 12.36 | 426.9821 | 426.9836 | 1.55 | 192.9895 | 342.9824 | | MPFNA | **2a** |
| (**14**) H-substituted PFCA ($n = 6$) |  | $C_8H_2F_{14}O_2$ | 13.30 | 394.9759 | 394.9772 | 1.34 | 118.9929 | 330.9800 | | MPFOA | **2a** |
| (**15**) PFCA-perfluoroalkyl-H-substituted-1DB ($n = 5$) | 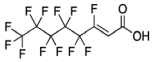 | $C_8H_2F_{12}O_2$ | 13.22 | 356.9793 | 356.9787 | 0.33 | 92.9958 | 142.9926 | 292.9816 | MPFOA | **2c** |
| (**16**) Perfluoroalkyl sulfonate ($n = 7$) |  | $C_7HF_{15}O_3S$ | 13.90 | 448.9334 | 448.9358 | 2.41 | 79.9576 | 98.9563 | 118.9931 | MPFOS | **2c** |

Table 1 (*Contd.*)

| Compound | Structure (linear isomer) | Formula | RT | Ref Mass | *m*/*z* | Δppm | MS/MS 1 | MS/MS 2 | MS/MS 3 | Surrogate | Confidence |
|---|---|---|---|---|---|---|---|---|---|---|---|
| (**17**) 8 : 2 FT carboxylic acid ($n = 8$) |  | $C_{10}H_3F_{17}O_2$ | 14.258 | 476.9789 | 476.9776 | 1.25 | 118.9902 | 242.9870 | 392.9763 | MPFDA | **1a** |
| (**18**) H-substituted-PFCA ($n = 7$) |  | $C_9H_2F_{16}O_2$ | 14.65 | 444.9727 | 444.9722 | 0.49 | 118.9932 | 380.9774 | | MPFNA | **2a** |
| (**19**) 9 : 2 FT carboxylic acid ($n = 9$) |  | $C_{11}H_3F_{19}O_2$ | 15.15 | 526.9757 | 526.9748 | 0.92 | 118.9932 | 292.9828 | 442.9734 | MPFDA | **2a** |
| (**20**) H-substituted-PFCA ($n = 8$) |  | $C_{10}H_2F_{18}O_2$ | 15.54 | 494.9694 | 494.9684 | 1.04 | 118.9932 | 168.9889 | 430.9732 | MPFDA | **2a** |
| (**21**) 10 : 2 FT carboxylic acid |  | $C_{12}H_3F_{21}O_2$ | 16.21 | 576.9725 | 576.972 | 0.73 | 118.9932 | 242.9860 | 492.9703 | MPFDA | **1a** |
| (**22**) H-substituted-PFCA ($n = 9$) |  | $C_{11}H_2F_{20}O_2$ | 16.76 | 544.9662 | 544.9664 | 0.18 | 118.9932 | 168.9890 | 480.9674 | MPFDA | **2a** |
| (**23**) 11 : 2 FT carboxylic acid | 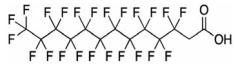 | $C_{13}H_3F_{23}O_2$ | 17.17 | 626.9693 | 626.9685 | 0.79 | 242.9880 | 342.9824 | 542.9716 | MPFDA | **2a** |
| (**24**) H-substituted-PFCA ($n = 10$) |  | $C_{12}H_2F_{22}O_2$ | 17.89 | 594.9631 | 594.9635 | 0.43 | 118.9928 | 168.9895 | 268.9836 | MPFDA | **2a** |

to the scale by Charbonnet *et al.*[92] Interestingly, significant in-source fragmentation was observed for the telomer acids, especially for the reference standards, which consisted of only the linear isomers. Fragmentation led to the loss of $CH_2O_2F_2$ for all FTCA standards. Overall, there is high confidence in the identity of the compounds listed in Table 1 based on signal strength, mass defect score, matching to an MS/MS library, identification by both FluoroMatch and NIST databases, and retention times predicted for homologous series.

Additional emerging PFAS were potentially identified out of the 74 high-quality features measured in MS/MS mode. These features had confidence levels below **3a** as they lacked a match to a library spectrum, had too few fragments, or had a S/N ratio < 200. Compounds with S/N > 100 and retention times that are reasonable based on retention times of standards ($n = 22$) are listed in Table S10.†

Most of the 24 emerging compounds identified with high confidence (Table 1) are H-substituted fluorinated carboxylic acids similar in chain length (C4–C12) to PFAS compounds on the EPA list. Incomplete fluorination and presence of odd chain lengths (*ex.* **13**, 7 : 2 FTCA) suggest the compounds were manufactured by electrochemical fluorination.[93] Curiously, many of the compounds had substantial amounts of branched isomers (see below), especially in the Wooster samples. The emerging compounds are different from aqueous film forming foam compositions reported in the literature.[31,94–96] FTCAs have been reported in precipitation elsewhere,[35,38,39] but to the best of our knowledge, this study marks the first detection in rainwater of H-PFCAs with a single F atom to H atom substitution. Furthermore, we present the first report of such highly branched FTCAs and H-PFCAs, so little is known about possible sources. Other emerging compounds identified with high confidence included PFAS with two carboxylate end groups and other compounds with H-substituted perfluorosulfonates. The additional 22 emerging PFAS compounds with lower confidence (Table S10†) showed a more diverse set of polar functional groups including sulfonates, thioether acetic acids, sulfonamides, and amines. It should be noted that most of the 22 compounds were at lower concentrations compared to the compounds listed in Table 1. However, if the identifications are accurate, these data indicate that a wide diversity of PFAS was found in the sampled precipitation.

The presence of the emerging PFAS compounds in precipitation may be linked to the manufacturing process and to volatility, which influences atmospheric mixing ratios. Vapor pressure increases as the chain length decreases and as the $pK_a$ of the acid group increases, allowing the neutral, more volatile species to form at a lower pH. Substitution of H for F near the carboxylate head group in PFCAs reduces electron induction effects and raises the $pK_a$ by ~2–3 units.[97] It may be that H-PFCAs are optimal for atmospheric deposition because they possess a $pK_a$ high enough to promote volatilization of the neutral protonated form and they are also acidic enough to promote dissolution in aqueous aerosol particles and cloud droplets.

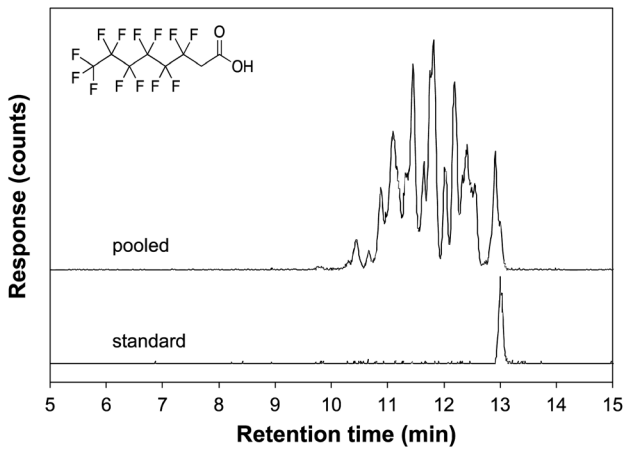


Fig. 1 Extracted ion chromatograms of *m*/*z* 376.9846 corresponding to compound **14** (6 : 2 FTCA) of the pooled sample (top) and the analytical standard (bottom) comprised of the linear isomer.

### Fluorocarbon chain length and branched isomers

Polyfluorinated carboxylic acids were the most commonly detected emerging PFAS in precipitation samples, particularly in the Wooster location. Compounds with even-length fluoroalkyl chains such as **11**, **17**, **21** (6 : 2 FTCA, 8 : 2 FTCA, and 10 : 2 FTCA, Table 1) are typically produced by telomerization, which due to the synthesis mechanism, results in linear carbon chains with even numbers of fluorinated carbon groups.[93,98] Similarly, the oxidation of fluorotelomer alcohols in the environment also results in the same even-numbered chain length speciation of PFCAs.[99] However, we found that precipitation samples had substantial amounts of odd chain length PFCAs, for example, compound **13**, 7 : 2 FTCA. Such findings are not indicative of an even chain length series that would be predicted for PFAS produced by fluorotelomerization. Odd chain length compounds were often at the same order of magnitude in concentration as the even chain length PFAS in the rainwater samples. For example, the relative ratios of the estimated concentrations of 6 : 2, 7 : 2, 8 : 2, 9 : 2, and 10 : 2 FTCA for the 5 June 2019 Wooster sample were 2.6 : 5.0 : 3.5 : 2.2 : 1.0, respectively. High concentrations of odd chain length compounds were consistent for samples at the Wooster location, with 7 : 2 FTCA sometimes having a concentration similar to even chain PFAS. The presence of odd chain lengths of PFAS may indicate other unknown local sources near the Wooster sampling site that contribute besides direct emission and deposition of fluorotelomer-derived products from the atmosphere.

Another notable observation was the large number of chromatographically distinct peaks observed for the emerging PFAS. For example, the extracted ion chromatogram (EIC) of the 376.9846 *m*/*z* ion corresponding to 6 : 2 FTCA has many peaks distributed across the retention time window of 10.5–13.2 min (Fig. 1). The peaks were attributed to branched isomers,[100] which typically have shorter retention times due to lower affinity of branched chains to the C18 stationary phase because steric effects reduce lipophilicity.[101,102] Interestingly, there were at least 11 chromatographic peaks for 6 : 2 FTCA, which may be due to

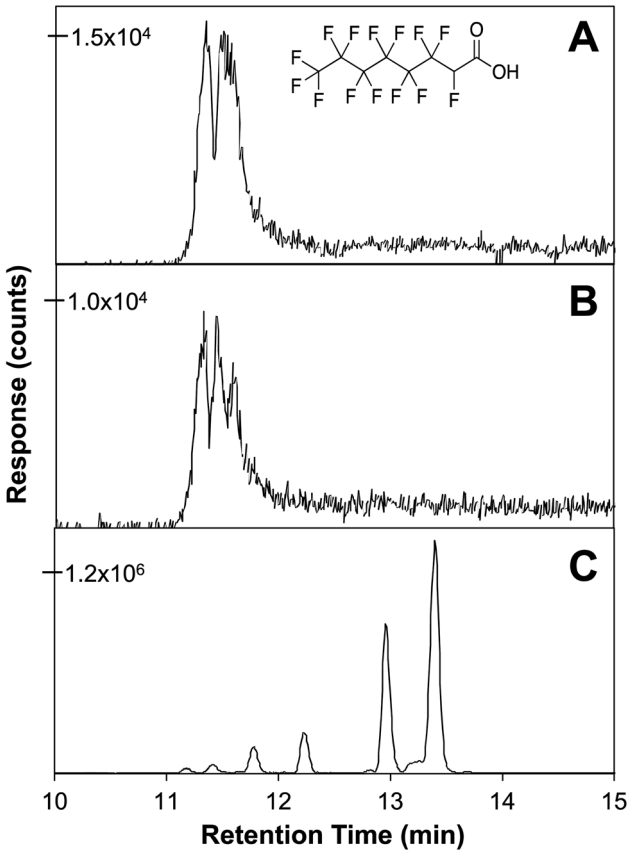


Fig. 2 Extracted ion chromatograms for $m/z$ 394.9759 corresponding to compound **11**, H-substituted PFCA from (A), Ashland, OH; (B), Rockford, OH; (C), Wooster OH.

both variations in the degree of branching and the position of the C–H groups relative to the carboxylate end group. The commercial standard for 6 : 2 FTCA (alternatively named 2-perfluorohexyl ethanoic acid) is the linear form, which can be used to verify the straight-chain isomer. Based upon the relative peak areas of the linear and branched forms, >70% of the 376.9846 $m/z$ ion feature in the pooled sample was present as putative branched isomers. This high degree of branching is uncharacteristic of PFAS manufactured by telomerization, where linear straight chain compounds are the predominant isoforms, nor does the profile match what is typically observed for PFCAs produced by ECF.[66] It was observed that the branched isomers in the precipitation samples exhibited less in-source fragmentation compared to the linear standards. Gas-phase dimerization was observed in the mass spectra of the linear FTCA standards, but was generally absent in the spectra of the putative branched features. We note that when calculating the amount of PFAS, the sum of peak areas for both the linear and branched forms was used in semi-quantification.

The peaks of the $m/z$ 376.9846 ion elute across a two-minute retention time window, which is a fairly broad elution profile. Nevertheless, we conclude that the peaks are isomers because they correspond to a single exact mass. Such a wide range is possible given that Pellizzaro *et al.*[102] determined that a C8 perfluorinated PFAS has 89 potential congeners. Substitution by H for one or more F atoms leads to substantially more congeners and structural diversity. One of the reasons for the substantial variation in retention times is the slowly changing solvent gradient used that is two times longer compared to previous reports.[103] The chemical interactions between a PFAS analyte and a non-polar stationary phase are not widely understood. The substitution of an H atom to various isomers appears to lead to substantial changes in affinity to the C18 stationary phase, potentially due to differences in polarity in parts of the PFAS structure or to steric effects. The unique chromatographic behavior of H-substituted emerging PFAS could be further studied in the future to better understand the properties of this class of molecules.

All of the H-substituted PFCA compounds identified in Table 1 showed multi-peak EICs characteristic of substantial amounts of branched isomers (ESI,† Appendix A). The distributions of the chromatographic peaks (and, by extension, the isomeric branching profiles) were evaluated with respect to sampling location and date. The chromatographic profile at Wooster was unique compared to other sites, where the EICs exhibited less overall abundance and fewer peaks at earlier retention times. For instance, compound **14**, a H-substituted analogue of PFOA ($m/z = 394.9772$) had five distinct peaks, whereas only the peaks with the shortest retention times were present in the chromatograms from samples at other sites (Fig. 2). At Wooster, the presumably branched isomer with the longer retention time dominated in terms of peak area. The isomeric profiles at Wooster in comparison to the profiles at the other sampling sites were consistent regardless of date, implying that location was the dominant factor controlling PFAS profiles. We hypothesize that Wooster is located in close proximity to a unique PFAS point source at the time of sampling, whereas the profiles at the other locations are more indicative of an average PFAS background. Moreover, background levels of H-substituted PFCAs appear more branched than the perfluorinated species. It is unknown why the more polar isomers are the predominant forms with high abundance in the diffuse regional background, perhaps due to long-term persistence and/or long-range transport. Further studies correlating the physical properties of emerging isomeric-rich PFAS and their fate and transport could be informative.[104]

EPA-list PFAS compounds showed much less branching compared to the emerging PFAS. For example, the branched fractions of PFOA (C8 perfluorinated carboxylic acid) and PFHxS (C6 perfluorinated sulfonic acid) comprised < 15% of the overall peak area (see Fig. S4 and S5†). The limited degree of PFOA branching is consistent with other literature reports testing precipitation samples.[24,27] Overall, the polyfluoro (H-substituted) compounds in our rainwater samples consisted primarily of branched isomers, whereas the perfluorinated compounds were primarily found as linear isomers. It is unknown if the differences in profile are due to source variation, to distinct transformation pathways, or to changes in physical properties (*e.g.*, p$K_a$) that alter partition ratios for the different classes of PFAS. However, these data suggest that further work is

 

sorely needed to better model the occurrence, fate, and transport of emerging PFAS.[41]

Both the high degree of branching among FTCA isomers and the presence of FTCAs with odd-numbered chain lengths in precipitation from Wooster suggest a unique localized point source during the sampling time period.[105] Thermal degradation of PFAS source compounds could explain the unique range of compounds detected at Wooster; however, recent literature reviews note that the thermal transformation processes of PFAS are poorly understood,[106,107] and data have indicated that PFAS destruction efficiencies depend upon structure, combustion chemistry, temperature, and operational conditions, such the presence or absence of oxygen.[108,109] Xiao *et al.*[110] studied the thermal stability and decomposition kinetics of PFAS from spent granular activated carbon during thermal regeneration. Interestingly, a PFOA thermal degradation intermediate with a precursor *m*/*z* of 395 and a fragment *m*/*z* of 119 was detected by low-resolution mass spectrometry.[110] This species could correspond to compound **14** (Table 1) found in our precipitation samples. It is critical to note that the source of additional PFAS detected at the Wooster site is unknown. However, the differences in emerging PFAS seen at Wooster indicate that PFAS can vary at the sub-regional scale.

### Concentrations and fluxes of PFAS in rainwater

Concentrations and deposition fluxes for the newly identified PFAS are given in Tables S11 and S12,† respectively, for the precipitation samples at each site. Concentrations in the blanks are given in Table S13.† The sum of all PFAS ($\Sigma_{PFAS}$) includes the ten PFAS quantified in Pike *et al.*[32] and the 22 PFAS semi-quantified in this work. (Compounds **22** and **24** from Table 1 are excluded from the analysis because of their high presence in method blanks). We refer to compounds as emerging if they do not appear in EPA Method 533 (ref. 111) and/or 537.1.[112]

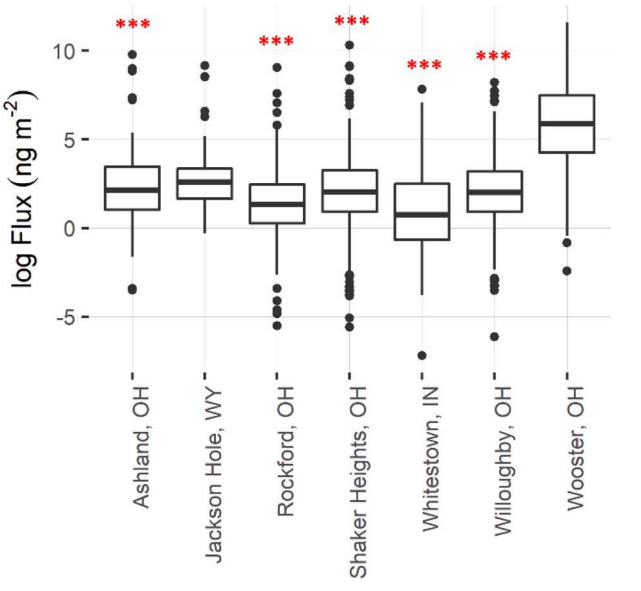


Fig. 3 Boxplot comparing the logarithm of the estimated PFAS deposition fluxes (in ng $m^{-2}$) of each compound and sampling date across each site. Red asterisks denote sampling sites with significantly different ($p < 0.05$) estimated deposition fluxes from Wooster, OH. Black points indicate outliers for each sampling site.

The most notable result from the semi-quantitative analysis is the anomalously high level of PFAS in rainwater from Wooster. To the best of our knowledge, H-PFCAs have never before been reported in precipitation, and the median concentrations and fluxes of $\Sigma_{H\text{-}PFCAs}$ are 782 ng $L^{-1}$ and 4.3 × $10^4$ ng $m^{-2}$, respectively, in Wooster. We also report the first published measurements of 8 : 2 FTCA, 10 : 2 FTCA, and 6 : 2 FTUCA in rainwater anywhere since 2010[35] (and in the United States since 1999).[38] Concentrations of these species in Ashland, Shaker Heights, Willoughby, and Rockford are on the same order as what has been seen elsewhere.[31,35,37,38] In contrast, concentrations in Wooster are higher by 1–2 orders of magnitude, as shown in Fig. S6.† The exceptionally high PFAS levels in rainwater from Wooster, coupled with the unique profiles discussed above, imply that a point source is likely present in the immediate vicinity of the sampling site. A previous study of the influence of point sources on PFAS deposition was conducted by Barton *et al.*,[22] who measured PFOA in rainwater collected in 2005 near a manufacturing plant that was actively using ammonium perfluorooctanoate. The authors found PFOA concentrations of 1660 ng $L^{-1}$ in rainwater collected at the manufacturing site, but the concentrations dropped to ~10 ng $L^{-1}$ at a distance of just 1 mile from the plant.[22] The median $\Sigma_{PFAS}$ concentration in our Wooster samples was 4450 ng $L^{-1}$, on the same order as the concentration of PFOA observed by Barton *et al.*[22] directly at the point source. The difference in PFAS levels at Wooster relative to the other Ohio/Indiana sites in our 2019 measurement campaign highlights the fact that sub-regional variations in PFAS deposition profiles are possible, presumably due to localized sources.

Regulations and restrictions surrounding PFAS use have certainly expanded since the 2005 measurements by Barton *et al.*[22] We no longer observe parts per billion levels of PFOA in rainwater samples, but we do see parts per billion levels of emerging PFAS in rainwater. Indeed, Fig. S6† shows that FTCA and FTUCA levels are even higher now than they were in prior decades. Although the absolute concentrations and fluxes in Table S11 and S12† are approximate because of the limitations of semi-quantitation, the values are still alarmingly high. In 2022, the U.S. EPA updated its lifetime health advisories for drinking water to just 0.004 ng $L^{-1}$ PFOA, 0.02 ng $L^{-1}$ PFOS, 0.01 ng $L^{-1}$ GenX (HFPO-DA), and 2000 ng $L^{-1}$ PFBS (C4 sulfonic acid).[113] With a maximum $\Sigma_{PFAS}$ concentration of 16 400 ng $L^{-1}$ in rainwater from Wooster, our results show that these advisories, while ambitious, are likely insufficient to mitigate PFAS intake, especially given the diversity of emerging PFAS now present in the environment.

### Statistical testing

Statistical testing was carried out to address whether PFAS profiles in Wooster were significantly different from profiles elsewhere with reference to class, functional group, or chain length. Comparisons between sites and PFAS class build on our

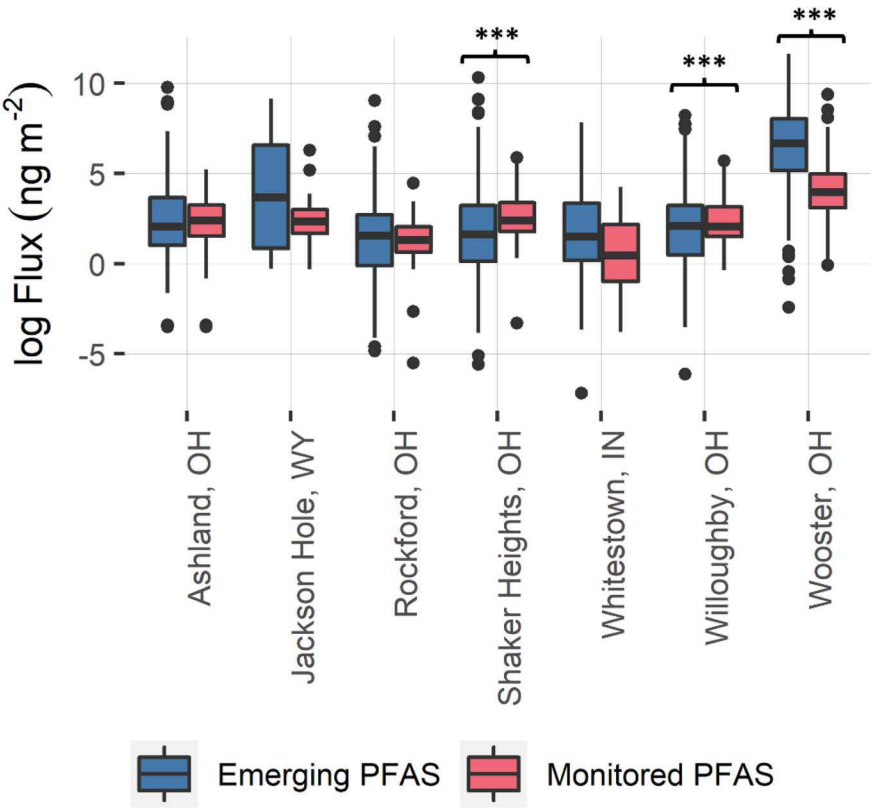


Fig. 4 Boxplot comparing log flux (in ng $m^{-2}$) of emerging and monitored PFAS at each site. Black asterisks indicate that emerging and monitored PFAS are statistically different ($p < 0.05$) at that site.

earlier statistical analysis,[32] which was limited to a subset of 10 PFAS (C2 and C4–C10 PFCAs, PFOS, and HFPO-DA) in precipitation. All statistical tests herein for samples compared estimated deposition fluxes instead of concentrations to remove influences of washout and scavenging, which cause PFAS concentrations to decrease over the course of a precipitation event.[16] We note that the estimated deposition fluxes integrate both wet and dry deposition over each sampling period, but dry deposition appeared to contribute a minor fraction of PFAS according to the site blanks in Table S13.† (Samples and blanks were compared using concentrations from Table S13† rather than fluxes because the method of calculating deposition fluxes through eqn (1) is restricted to precipitation events and cannot be extended to blanks). Finally, we acknowledge that the estimated deposition fluxes bear inherent uncertainty because of the semiquantitative nature of suspect screening and non-targeted analysis. Nevertheless, Kruskal–Wallis tests, Kendall's tau correlations, and PCA can provide insight into trends within the data set.

**Overall deposition flux.** A Kruskal–Wallis test was used to compare estimated deposition fluxes of all PFAS across sampling sites (Fig. 3). As anticipated, deposition of PFAS in Wooster was significantly different from deposition at most other sampling sites. All other sites showed no statistical difference in estimated deposition fluxes. The significantly greater flux in Wooster suggests that a local point of PFAS contamination is likely present.

**EPA monitoring status.** In this work, suspect screening and a non-targeted approach allowed for 23 emerging PFAS to be identified with high confidence (Table 1, excluding EPA-monitored compound **16**). Fig. 4 compares the estimated deposition flux of EPA-monitored PFAS and emerging PFAS at each site. Shaker Heights, Willoughby, and Wooster displayed significantly different estimated deposition fluxes when comparing EPA-monitored and emerging PFAS according to a Kruskal–Wallis test (Table S14†). At each site, estimated deposition fluxes of emerging PFAS exceeded those of EPA-monitored PFAS. Indeed, our results likely underestimate the PFAS fraction in rainwater comprised by emerging compounds because we did not quantify the additional 23 emerging PFAS in Table S10† that had lower identification confidence (levels 3c and d, 4, and 5a and b).[92]

**Chain length.** According to a Kruskal–Wallis test for chain length and site location, several sites had significantly different levels (Table S15 and S16†) of ultra-short PFAS (C2–C3) in comparison to short-chain (C4–C7) and long-chain (≥C8) PFAS. As shown in Fig. S7,† the estimated deposition fluxes of ultra-short PFAS greatly exceeded the estimated deposition fluxes of other PFAS detected in the precipitation samples collected at Ashland, Jackson Hole, and Shaker Heights. This trend matches earlier measurements of trifluoroacetic acid (TFA, C2) and PFPrA (C3) in rainwater in which the concentrations of ultra-short PFCAs greatly exceeded the concentrations of longer-chain PFCAs.[26,31,32,38,39,114] The ultra-short chain PFAS are likely

 

present in precipitation at such high levels because these small molecules have higher vapor pressures and are more water-soluble than longer-chain PFAS. Accordingly, TFA and PFPrA are more likely to enter the atmosphere through volatilization and subsequently partition into aqueous aerosol particles or cloud droplets. Furthermore, ultra-short PFAS are readily formed from reactions of other fluorinated species, such as longer-chain PFAS or from the hydrochlorofluorocarbons (HCFCs) and hydrofluorocarbons (HFCs) used as refrigerants.[2,115] TFA in particular is ubiquitous in all compartments of the environment, including rainwater.[115–117]

**Functional class.** A Kruskal–Wallis test for functional class and location indicated that each sampling site displayed significant differences in PFAS profile according to functional class. Notably, the estimated deposition fluxes of FTCAs and H-PFCAs at Wooster are significantly greater than the fluxes of most other functional classes (Fig. S8 and Table S17 and S18†). In a related analysis, Fig. S9† illustrates differences in estimated deposition flux for each functional class across all sampling sites. Wooster had a significantly different deposition profile of FTCAs, FTUCAs, H-PFCAs, H-PFdiCAs, oPFSAs, and PFCAs when compared to all other sampling sites (see Table S19 and S20† for data and Table S1† for acronyms). The differences in estimated deposition are particularly interesting for the sites located in close proximity. As shown in Fig. S1,† Shaker Heights, Rockford, Ashland, and Willoughby are all located within 280 km of Wooster. The differences in functional class profiles found in precipitation at these sites further support the hypothesis that elevated PFAS deposition in Wooster is a localized phenomenon.

**PFAS correlations.** Kendall's tau correlation was employed to examine the relationship between the estimated deposition fluxes of individual PFAS at each site. Table S21† highlights particularly strong correlations ($\tau > 0.80$). PFAS with strong positive correlations may have originated from the same source, though origins cannot be proved through correlations alone. Wooster had the greatest number of correlations between compounds, which can be divided into the two distinct groups listed in Table S22.† First, compounds **1**, **2**, **3**, and **12** (Group A) were all strongly and positively correlated to one another. Functional classes of the Group A PFAS vary; however, three of the four PFAS are short-chain, while the fourth is ultra-short. Group B consists of 15 PFAS. Again, the functional classes of these compounds vary greatly, but all have a long chain length. The A and B groupings, which are defined by their strong correlations and chain lengths, suggest short-chain and long-chain PFAS detected in Wooster could have different origins—either different emission sources or different atmospheric formation routes.

**Principal component analysis.** Principal component analysis was performed on the precipitation samples to visualize similarities between sample compositions, again with the goal of gaining insight into PFAS origins. The first principal component (PC1) explains 96% of the variation in the data, while the second principal component (PC2) accounts for 3% of the variation (Fig. S10†). The cumulative variation explained by the first two components is 99%.

Fig. S11† clearly shows the anomalous nature of the samples collected in Wooster. While all other samples lie primarily in proximity to zero in PC1, the samples from Wooster are more distributed along this axis. PC1 was strongly correlated (coefficient > 0.90) to 25 PFAS (see Table S23†). The estimated deposition fluxes of these compounds distinguished Wooster from other sampling sites. In addition, the sample collected in Wooster on 6 July 2019 is vastly different from all other samples and is clearly visible in Fig. S11† as an outlier along PC1. This particular date was a key focus of our air mass back trajectory analysis, discussed later. Along PC2, sites other than Wooster displayed more spatial variability in Fig. S11.† TFA, PFHpS (**16**), and HFPO-DA most significantly contributed to PC2, suggesting that the deposition of these compounds across sites varies widely. In summary, PCA clearly highlights yet again the anomalous deposition flux of PFAS in Wooster.

### Air mass back trajectories

We turned to air mass back trajectories for further site-specific insights into whether regional atmospheric transport affected PFAS deposition profiles. The frequency plots in Appendix B of the ESI† show regions where the majority of air masses have crossed. In general, air masses approached the collection sites from the west. At each site, we compared back trajectories on days with high PFAS levels (defined as $\Sigma_{PFAS} > 50\%$ of the maximum $\Sigma_{PFAS}$ deposition flux) and on days with low PFAS levels (defined as $\Sigma_{PFAS} \leq 50\%$ of the maximum $\Sigma_{PFAS}$ deposition flux). For most Ohio sites, days with elevated PFAS levels exhibited more influence from air masses passing over Michigan: more than 25% of trajectories crossed Michigan on high PFAS days in Ashland, Shaker Heights, Rockford, and Willoughby. Southwestern influences also contributed to air masses on elevated PFAS deposition days: more than 25% of trajectories crossed western Illinois on high PFAS days in Rockford, and more than 25% of trajectories crossed Arkansas, Missouri, and Illinois on high PFAS days in Ashland and Wooster. We caution that air mass back trajectories are not direct indications of PFAS origins; rather, the frequency plots in Appendix B are intended to simply illustrate patterns in meteorological conditions. Although it is reasonable to detect high PFAS levels in precipitation from air masses that have crossed Michigan, where PFAS contamination from industrial activities is well-established,[118] such evidence is circumstantial for rainwater from the Ohio sites. Insufficient samples were collected to identify trends in air mass trajectories at Jackson Hole, WY or Whitestown, IN.

Curiously, PFAS levels in precipitation from Wooster were about an order of magnitude higher in the 6 July 2019 sample than in any other sample. The estimated total PFAS deposition flux and total concentration were $7.48 \times 10^5$ ng m$^{-2}$ and $1.82 \times 10^4$ ng L$^{-1}$, respectively, on July 6$^{th}$ in comparison to median values of $4.41 \times 10^4$ ng m$^{-2}$ and $4.69 \times 10^3$ ng L$^{-1}$ for the Wooster site overall. Even though the July 6$^{th}$ sample from Wooster was an egregious outlier on the PCA plot (Fig. S11†), the air mass frequency map for July 6 showed roughly the same patterns as the maps on the other nine sampling dates in

Wooster (see Fig. B7 in the ESI†). We conclude that, at least at the Wooster site, local sources dominated over background deposition of PFAS from atmospheric transport.

## Conclusions

Data here show that emerging compounds may make up a majority of total PFAS load in precipitation and potentially elsewhere in the environment if cumulative deposition from the atmosphere is significant. However, instrumentation to conduct high-resolution mass spectral analysis is not widely accessible for routine testing, and data analysis is time-consuming.[63] Further measurements of emerging PFAS can be used to generate targeted analyte lists of representative compounds that, in conjunction with legacy monitored analytes, should more accurately estimate total PFAS fluxes. Branched isomers also require further study. The chromatographically distinct mixtures of PFAS observed in non-targeted analysis highlight the need for a wider range of PFAS standards. Standards that include branched isomers would be especially helpful to confirm the identity of mass-identical, chromatographically distinct features, which would subsequently improve the understanding of PFAS mixtures for source identification. The structural complexity of the emerging PFAS detected also suggests a need for improved structural databases of manufactured fluorochemicals. In addition, understanding how fluorochemicals are chemically transformed, either by an industrial process or through reactions in the atmosphere, may be useful to explain the structural diversity of PFAS detected in precipitation. Toxicological data should be collected to understand the risks of the emerging PFAS. If the high concentration of emerging PFAS in Wooster, OH is due to incomplete incineration of PFAS, then the data highlight the critical need to study and optimize thermal mechanisms to mineralize PFAS and prevent emission of fluorochemicals.

## Conflicts of interest

There are no conflicts to declare.

## Acknowledgements

This work was supported by the National Science Foundation (Grant Number CHE-2017788), by the Strategic Environmental Research and Development Program (Grant Number ER13-1800), and by The College of Wooster Copeland Fund. The authors would like to thank Judy Amburgey-Peters, Betsy Bernfeld, Claire Hefner, the Pikes, the Sapps, and the Sutherlands for collecting water samples.

## References

1 J. Glüge, M. Scheringer, I. T. Cousins, J. C. DeWitt, G. Goldenman, D. Herzke, R. Lohmann, C. A. Ng, X. Trier and Z. Wang, An overview of the uses of per- and polyfluoroalkyl substances (PFAS), *Environ. Sci.: Processes Impacts*, 2020, **22**, 2345–2373.

2 C. J. Young and S. A. Mabury, in *Reviews of Environmental Contamination and Toxicology*, ed. P. De Voogt, Springer New York, New York, NY, 2010, vol. 208, pp. 1–109.

3 A. B. Radi, K. E. Noll and A. K. Oskouie, Per- and Polyfluoroalkyl Substances: Background Information with Focus on Modeling of Fate and Transport of Per- and Polyfluroalkyl Substances in Air Media, *J. Environ. Eng.*, 2022, **148**, 03122001.

4 J. M. Armitage, U. Schenker, M. Scheringer, J. W. Martin, M. MacLeod and I. T. Cousins, Modeling the Global Fate and Transport of Perfluorooctane Sulfonate (PFOS) and Precursor Compounds in Relation to Temporal Trends in Wildlife Exposure, *Environ. Sci. Technol.*, 2009, **43**, 9274–9280.

5 J. J. MacInnis, I. Lehnherr, D. C. G. Muir, K. A. St. Pierre, V. L. St. Louis, C. Spencer and A. O. De Silva, Fate and Transport of Perfluoroalkyl Substances from Snowpacks into a Lake in the High Arctic of Canada, *Environ. Sci. Technol.*, 2019, **53**, 10753–10762.

6 C. P. Thackray, N. E. Selin and C. J. Young, A global atmospheric chemistry model for the fate and transport of PFCAs and their precursors, *Environ. Sci.: Processes Impacts*, 2020, **22**, 285–293.

7 B. Sha, J. H. Johansson, P. Tunved, P. Bohlin-Nizzetto, I. T. Cousins and M. E. Salter, Sea Spray Aerosol (SSA) as a Source of Perfluoroalkyl Acids (PFAAs) to the Atmosphere: Field Evidence from Long-Term Air Monitoring, *Environ. Sci. Technol.*, 2022, **56**, 228–238.

8 J. A. Faust, PFAS on atmospheric aerosol particles: a review, *Environ. Sci.: Processes Impacts*, 2022, DOI: **10.1039/D2EM00002D**.

9 I. T. Cousins, J. H. Johansson, M. E. Salter, B. Sha and M. Scheringer, Outside the Safe Operating Space of a New Planetary Boundary for Per- and Polyfluoroalkyl Substances (PFAS), *Environ. Sci. Technol.*, 2022, **56**, 11172–11179.

10 C. J. Young, V. I. Furdui, J. Franklin, R. M. Koerner, D. C. G. Muir and S. A. Mabury, Perfluorinated Acids in Arctic Snow: New Evidence for Atmospheric Formation, *Environ. Sci. Technol.*, 2007, **41**, 3455–3461.

11 N. L. Stock, V. I. Furdui, D. C. G. Muir and S. A. Mabury, Perfluoroalkyl Contaminants in the Canadian Arctic: Evidence of Atmospheric Transport and Local Contamination, *Environ. Sci. Technol.*, 2007, **41**, 3529–3536.

12 C. M. Butt, U. Berger, R. Bossi and G. T. Tomy, Levels and trends of poly- and perfluorinated compounds in the arctic environment, *Sci. Total Environ.*, 2010, **408**, 2936–2965.

13 L. Ahrens, M. Shoeib, S. Del Vento, G. Codling and C. Halsall, Polyfluoroalkyl compounds in the Canadian Arctic atmosphere, *Environ. Chem.*, 2011, **8**, 399–406.

14 P. Casal, Y. Zhang, J. W. Martin, M. Pizarro, B. Jiménez and J. Dachs, Role of Snow Deposition of Perfluoroalkylated Substances at Coastal Livingston Island (Maritime Antarctica), *Environ. Sci. Technol.*, 2017, **51**, 8460–8470.

 

15 G. Casas, A. Martinez-Varela, M. Vila-Costa, B. Jiménez and J. Dachs, Rain Amplification of Persistent Organic Pollutants, *Environ. Sci. Technol.*, 2021, **55**, 12961–12972.
16 S. Taniyasu, N. Yamashita, H.-B. Moon, K. Y. Kwok, P. K. S. Lam, Y. Horii, G. Petrick and K. Kannan, Does wet precipitation represent local and regional atmospheric transportation by perfluorinated alkyl substances?, *Environ. Int.*, 2013, **55**, 25–32.
17 E. M. Sunderland, X. C. Hu, C. Dassuncao, A. K. Tokranov, C. C. Wagner and J. G. Allen, A review of the pathways of human exposure to poly- and perfluoroalkyl substances (PFASs) and present understanding of health effects, *J. Exposure Sci. Environ. Epidemiol.*, 2019, **29**, 131–147.
18 S. E. Fenton, A. Ducatman, A. Boobis, J. C. DeWitt, C. Lau, C. Ng, J. S. Smith and S. M. Roberts, Per- and Polyfluoroalkyl Substance Toxicity and Human Health Review: Current State of Knowledge and Strategies for Informing Future Research, *Environ. Toxicol. Chem.*, 2021, **40**, 606–630.
19 A. O. De Silva, J. M. Armitage, T. A. Bruton, C. Dassuncao, W. Heiger-Bernays, X. C. Hu, A. Kärrman, B. Kelly, C. Ng, A. Robuck, M. Sun, T. F. Webster and E. M. Sunderland, PFAS Exposure Pathways for Humans and Wildlife: A Synthesis of Current Knowledge and Key Gaps in Understanding, *Environ. Toxicol. Chem.*, 2021, **40**, 631–657.
20 G. T. Ankley, P. Cureton, R. A. Hoke, M. Houde, A. Kumar, J. Kurias, R. Lanno, C. McCarthy, J. Newsted, C. J. Salice, B. E. Sample, M. S. Sepúlveda, J. Steevens and S. Valsecchi, Assessing the Ecological Risks of Per- and Polyfluoroalkyl Substances: Current State-of-the Science and a Proposed Path Forward, *Environ. Toxicol. Chem.*, 2021, **40**, 564–605.
21 M. G. Evich, M. J. B. Davis, J. P. McCord, B. Acrey, J. A. Awkerman, D. R. U. Knappe, A. B. Lindstrom, T. F. Speth, C. Tebes-Stevens, M. J. Strynar, Z. Wang, E. J. Weber, W. M. Henderson and J. W. Washington, Per- and polyfluoroalkyl substances in the environment, *Science*, 2022, **375**, eabg9065.
22 C. A. Barton, M. A. Kaiser and M. H. Russell, Partitioning and removal of perfluorooctanoate during rain events: the importance of physical–chemical properties, *J. Environ. Monit.*, 2007, **9**, 839–846.
23 W. Liu, Y. Jin, X. Quan, K. Sasaki, N. Saito, S. F. Nakayama, I. Sato and S. Tsuda, Perfluorosulfonates and perfluorocarboxylates in snow and rain in Dalian, China, *Environ. Int.*, 2009, **35**, 737–742.
24 J. H. Johansson, Y. Shi, M. Salter and I. T. Cousins, Spatial variation in the atmospheric deposition of perfluoroalkyl acids: source elucidation through analysis of isomer patterns, *Environ. Sci.: Processes Impacts*, 2018, **20**, 997–1006.
25 M. Chen, C. Wang, K. Gao, X. Wang, J. Fu, P. Gong and Y. Wang, Perfluoroalkyl substances in precipitation from the Tibetan Plateau during monsoon season: concentrations, source regions and mass fluxes, *Chemosphere*, 2021, **282**, 131105.
26 B. F. Scott, C. A. Moody, C. Spencer, J. M. Small, D. C. G. Muir and S. A. Mabury, Analysis for Perfluorocarboxylic Acids/Anions in Surface Waters and Precipitation Using GC-MS and Analysis of PFOA from Large-Volume Samples, *Environ. Sci. Technol.*, 2006, **40**, 6405–6410.
27 A. O. De Silva, D. C. G. Muir and S. A. Mabury, Distribution of Perfluorocarboxylate Isomers in Select Samples from the North American Environment, *Environ. Toxicol. Chem.*, 2009, **28**, 1801–1814.
28 S. B. Gewurtz, L. E. Bradley, S. Backus, A. Dove, D. McGoldrick, H. Hung and H. Dryfhout-Clark, Perfluoroalkyl Acids in Great Lakes Precipitation and Surface Water (2006–2018) Indicate Response to Phase-outs, Regulatory Action, and Variability in Fate and Transport Processes, *Environ. Sci. Technol.*, 2019, **53**, 8543–8552.
29 C. E. Müller, N. Spiess, A. C. Gerecke, M. Scheringer and K. Hungerbühler, Quantifying Diffuse and Point Inputs of Perfluoroalkyl Acids in a Nonindustrial River Catchment, *Environ. Sci. Technol.*, 2011, **45**, 9901–9909.
30 G. Sammut, E. Sinagra, R. Helmus and P. de Voogt, Perfluoroalkyl substances in the Maltese environment – (I) surface water and rain water, *Sci. Total Environ.*, 2017, **589**, 182–190.
31 S. Taniyasu, K. Kannan, L. W. Y. Yeung, K. Y. Kwok, P. K. S. Lam and N. Yamashita, Analysis of trifluoroacetic acid and other short-chain perfluorinated acids (C2–C4) in precipitation by liquid chromatography–tandem mass spectrometry: comparison to patterns of long-chain perfluorinated acids (C5–C18), *Anal. Chim. Acta*, 2008, **619**, 221–230.
32 K. A. Pike, P. L. Edmiston, J. J. Morrison and J. A. Faust, Correlation Analysis of Perfluoroalkyl Substances in Regional U.S. Precipitation Events, *Water Res.*, 2021, **190**, 116685.
33 M. S. Shimizu, R. Mott, A. Potter, J. Zhou, K. Baumann, J. D. Surratt, B. Turpin, G. B. Avery, J. Harfmann, R. J. Kieber, R. N. Mead, S. A. Skrabal and J. D. Willey, Atmospheric Deposition and Annual Flux of Legacy Perfluoroalkyl Substances and Replacement Perfluoroalkyl Ether Carboxylic Acids in Wilmington, NC, USA, *Environ. Sci. Technol. Lett.*, 2021, **8**, 366–372.
34 K. Y. Kwok, S. Taniyasu, L. W. Y. Yeung, M. B. Murphy, P. K. S. Lam, Y. Horii, K. Kannan, G. Petrick, R. K. Sinha and N. Yamashita, Flux of Perfluorinated Chemicals through Wet Deposition in Japan, the United States, And Several Other Countries, *Environ. Sci. Technol.*, 2010, **44**, 7043–7049.
35 L. Zhao, M. Zhou, T. Zhang and H. Sun, Polyfluorinated and Perfluorinated Chemicals in Precipitation and Runoff from Cities Across Eastern and Central China, *Arch. Environ. Contam. Toxicol.*, 2013, **64**, 198–207.
36 A. Dreyer, V. Matthias, I. Weinberg and R. Ebinghaus, Wet deposition of poly- and perfluorinated compounds in Northern Germany, *Environ. Pollut.*, 2010, **158**, 1221–1227.
37 M. Loewen, T. Halldorson, F. Wang and G. Tomy, Fluorotelomer Carboxylic Acids and PFOS in Rainwater

from an Urban Center in Canada, *Environ. Sci. Technol.*, 2005, **39**, 2944–2951.

38 B. F. Scott, C. Spencer, S. A. Mabury and D. C. G. Muir, Poly and Perfluorinated Carboxylates in North American Precipitation, *Environ. Sci. Technol.*, 2006, **40**, 7167–7174.

39 H. Chen, L. Zhang, M. Li, Y. Yao, Z. Zhao, G. Munoz and H. Sun, Per- and polyfluoroalkyl substances (PFASs) in precipitation from mainland China: Contributions of unknown precursors and short-chain (C2–C3) perfluoroalkyl carboxylic acids, *Water Res.*, 2019, **153**, 169–177.

40 J. P. Koelmel, P. Stelben, C. A. McDonough, D. A. Dukes, J. J. Aristizabal-Henao, S. L. Nason, Y. Li, S. Sternberg, E. Lin, M. Beckmann, A. J. Williams, J. Draper, J. P. Finch, J. K. Munk, C. Deigl, E. E. Rennie, J. A. Bowden and K. J. Godri Pollitt, FluoroMatch 2.0—making automated and comprehensive non-targeted PFAS annotation a reality, *Anal. Bioanal. Chem.*, 2022, **414**, 1201–1215.

41 Z. Wang, J. C. DeWitt, C. P. Higgins and I. T. Cousins, A Never-Ending Story of Per- and Polyfluoroalkyl Substances (PFASs)?, *Environ. Sci. Technol.*, 2017, **51**, 2508–2518.

42 Z. Wang, A. M. Buser, I. T. Cousins, S. Demattio, W. Drost, O. Johansson, K. Ohno, G. Patlewicz, A. M. Richard, G. W. Walker, G. S. White and E. Leinala, A New OECD Definition for Per- and Polyfluoroalkyl Substances, *Environ. Sci. Technol.*, 2021, **55**, 15575–15578.

43 M. Sun, E. Arevalo, M. Strynar, A. Lindstrom, M. Richardson, B. Kearns, A. Pickett, C. Smith and D. R. U. Knappe, Legacy and Emerging Perfluoroalkyl Substances Are Important Drinking Water Contaminants in the Cape Fear River Watershed of North Carolina, *Environ. Sci. Technol. Lett.*, 2016, **3**, 415–419.

44 T. Ruan and G. Jiang, Analytical methodology for identification of novel per- and polyfluoroalkyl substances in the environment, *TrAC, Trends Anal. Chem.*, 2017, **95**, 122–131.

45 R. A. Brase, E. J. Mullin and D. C. Spink, Legacy and Emerging Per- and Polyfluoroalkyl Substances: Analytical Techniques, Environmental Fate, and Health Effects, *Int. J. Mol. Sci.*, 2021, **22**, 995.

46 M. Liu, G. Munoz, S. Vo Duy, S. Sauvé and J. Liu, Per- and Polyfluoroalkyl Substances in Contaminated Soil and Groundwater at Airports: A Canadian Case Study, *Environ. Sci. Technol.*, 2022, **56**, 885–895.

47 Y. Liu, L. A. D'Agostino, G. Qu, G. Jiang and J. W. Martin, High-resolution mass spectrometry (HRMS) methods for nontarget discovery and characterization of poly- and per-fluoroalkyl substances (PFASs) in environmental and human samples, *TrAC, Trends Anal. Chem.*, 2019, **121**, 115420.

48 J. L. Guelfo, S. Korzeniowski, M. A. Mills, J. Anderson, R. H. Anderson, J. A. Arblaster, J. M. Conder, I. T. Cousins, K. Dasu, B. J. Henry, L. S. Lee, J. Liu, E. R. McKenzie and J. Willey, Environmental Sources, Chemistry, Fate, and Transport of Per- and Polyfluoroalkyl Substances: State of the Science, Key Knowledge Gaps, and Recommendations Presented at the August 2019 SETAC Focus Topic Meeting, *Environ. Toxicol. Chem.*, 2021, **40**, 3234–3260.

49 S. Jia, M. Marques Dos Santos, C. Li and S. A. Snyder, Recent advances in mass spectrometry analytical techniques for per- and polyfluoroalkyl substances (PFAS), *Anal. Bioanal. Chem.*, 2022, **414**, 2795–2807.

50 J. Aceña, S. Stampachiacchiere, S. Pérez and D. Barceló, Advances in liquid chromatography–high-resolution mass spectrometry for quantitative and qualitative environmental analysis, *Anal. Bioanal. Chem.*, 2015, **407**, 6289–6299.

51 B. González-Gaya, N. Lopez-Herguedas, D. Bilbao, L. Mijangos, A. M. Iker, N. Etxebarria, M. Irazola, A. Prieto, M. Olivares and O. Zuloaga, Suspect and non-target screening: the last frontier in environmental analysis, *Anal. Methods*, 2021, **13**, 1876–1904.

52 S. Newton, R. McMahen, J. A. Stoeckel, M. Chislock, A. Lindstrom and M. Strynar, Novel Polyfluorinated Compounds Identified Using High Resolution Mass Spectrometry Downstream of Manufacturing Facilities near Decatur, Alabama, *Environ. Sci. Technol.*, 2017, **51**, 1544–1552.

53 J. P. McCord, M. J. Strynar, J. W. Washington, E. L. Bergman and S. M. Goodrow, Emerging Chlorinated Polyfluorinated Polyether Compounds Impacting the Waters of Southwestern New Jersey Identified by Use of Nontargeted Analysis, *Environ. Sci. Technol. Lett.*, 2020, **7**, 903–908.

54 S. Yukioka, S. Tanaka, Y. Suzuki, S. Echigo, A. Kärrman and S. Fujii, A profile analysis with suspect screening of per- and polyfluoroalkyl substances (PFASs) in firefighting foam impacted waters in Okinawa, Japan, *Water Res.*, 2020, **184**, 116207.

55 R. Gonzalez de Vega, A. Cameron, D. Clases, T. M. Dodgen, P. A. Doble and D. P. Bishop, Simultaneous targeted and non-targeted analysis of per- and polyfluoroalkyl substances in environmental samples by liquid chromatography-ion mobility-quadrupole time of flight-mass spectrometry and mass defect analysis, *J. Chromatogr. A*, 2021, **1653**, 462423.

56 J. Yao, N. Sheng, Y. Guo, L. W. Y. Yeung, J. Dai and Y. Pan, Nontargeted Identification and Temporal Trends of Per- and Polyfluoroalkyl Substances in a Fluorochemical Industrial Zone and Adjacent Taihu Lake, *Environ. Sci. Technol.*, 2022, **56**, 7986–7996.

57 Y. Wang, N. Yu, X. Zhu, H. Guo, J. Jiang, X. Wang, W. Shi, J. Wu, H. Yu and S. Wei, Suspect and Nontarget Screening of Per- and Polyfluoroalkyl Substances in Wastewater from a Fluorochemical Manufacturing Park, *Environ. Sci. Technol.*, 2018, **52**, 11007–11016.

58 P. Jacob, K. A. Barzen-Hanson and D. E. Helbling, Target and Nontarget Analysis of Per- and Polyfluoroalkyl Substances in Wastewater from Electronics Fabrication Facilities, *Environ. Sci. Technol.*, 2021, **55**, 2346–2356.

59 X. Wang, N. Yu, Y. Qian, W. Shi, X. Zhang, J. Geng, H. Yu and S. Wei, Non-target and suspect screening of per- and polyfluoroalkyl substances in Chinese municipal wastewater treatment plants, *Water Res.*, 2020, **183**, 115989.

 

60 Y. Jeong, K. M. Da Silva, E. Iturrospe, Y. Fuiji, T. Boogaerts, A. L. N. van Nuijs, J. Koelmel and A. Covaci, Occurrence and contamination profile of legacy and emerging per- and polyfluoroalkyl substances (PFAS) in Belgian wastewater using target, suspect and non-target screening approaches, *J. Hazard. Mater.*, 2022, **437**, 129378.

61 N. Yu, H. Guo, J. Yang, L. Jin, X. Wang, W. Shi, X. Zhang, H. Yu and S. Wei, Non-Target and Suspect Screening of Per- and Polyfluoroalkyl Substances in Airborne Particulate Matter in China, *Environ. Sci. Technol.*, 2018, **52**, 8205–8214.

62 N. Yu, H. Wen, X. Wang, E. Yamazaki, S. Taniyasu, N. Yamashita, H. Yu and S. Wei, Nontarget Discovery of Per- and Polyfluoroalkyl Substances in Atmospheric Particulate Matter and Gaseous Phase Using Cryogenic Air Sampler, *Environ. Sci. Technol.*, 2020, **54**, 3103–3113.

63 M. J. Benotti, L. A. Fernandez, G. F. Peaslee, G. S. Douglas, A. D. Uhler and S. Emsbo-Mattingly, A forensic approach for distinguishing PFAS materials, *Environ. Forensics*, 2020, **21**, 319–333.

64 J. A. Charbonnet, A. E. Rodowa, N. T. Joseph, J. L. Guelfo, J. A. Field, G. D. Jones, C. P. Higgins, D. E. Helbling and E. F. Houtz, Environmental Source Tracking of Per- and Polyfluoroalkyl Substances within a Forensic Context: Current and Future Techniques, *Environ. Sci. Technol.*, 2021, **55**, 7237–7245.

65 J. P. Benskin, A. O. De Silva and J. W. Martin, in *Reviews of Environmental Contamination and Toxicology Volume 208*, ed. P. De Voogt, Springer New York, New York, NY, 2010, vol. 208, pp. 111–160.

66 K. Schulz, M. R. Silva and R. Klaper, Distribution and effects of branched *versus* linear isomers of PFOA, PFOS, and PFHxS: a review of recent literature, *Sci. Total Environ.*, 2020, **733**, 139186.

67 S. Rayne, K. Forest and K. J. Friesen, Estimated congener specific gas-phase atmospheric behavior and fractionation of perfluoroalkyl compounds: rates of reaction with atmospheric oxidants, air–water partitioning, and wet/dry deposition lifetimes, *J. Environ. Sci. Health, Part A*, 2009, **44**, 936–954.

68 D. D. Perrin, B. Dempsey and E. P. Serjeant, *pKa Prediction for Organic Acids and Bases*, Springer Netherlands, Dordrecht, 1981.

69 D. C. Burns, D. A. Ellis, H. Li, C. J. McMurdo and E. Webster, Experimental p$K_a$ Determination for Perfluorooctanoic Acid (PFOA) and the Potential Impact of p$K_a$ Concentration Dependence on Laboratory-Measured Partitioning Phenomena and Environmental Modeling, *Environ. Sci. Technol.*, 2008, **42**, 9283–9288.

70 Z. Wang, M. MacLeod, I. T. Cousins, M. Scheringer and K. Hungerbühler, Using COSMOtherm to predict physicochemical properties of poly- and perfluorinated alkyl substances (PFASs), *Environ. Chem.*, 2011, **8**, 389–398.

71 A. Kärrman, K. Elgh-Dalgren, C. Lafossas and T. Møskeland, Environmental levels and distribution of structural isomers of perfluoroalkyl acids after aqueous fire-fighting foam (AFFF) contamination, *Environ. Chem.*, 2011, **8**, 372–380.

72 X. Chen, L. Zhu, X. Pan, S. Fang, Y. Zhang and L. Yang, Isomeric specific partitioning behaviors of perfluoroalkyl substances in water dissolved phase, suspended particulate matters and sediments in Liao River Basin and Taihu Lake, China, *Water Res.*, 2015, **80**, 235–244.

73 Y. Gao, Y. Liang, K. Gao, Y. Wang, C. Wang, J. Fu, Y. Wang, G. Jiang and Y. Jiang, Levels, spatial distribution and isomer profiles of perfluoroalkyl acids in soil, groundwater and tap water around a manufactory in China, *Chemosphere*, 2019, **227**, 305–314.

74 S. Fang, B. Sha, H. Yin, Y. Bian, B. Yuan and I. T. Cousins, Environment occurrence of perfluoroalkyl acids and associated human health risks near a major fluorochemical manufacturing park in southwest of China, *J. Hazard. Mater.*, 2020, **396**, 122617.

75 H. A. Langberg, H. P. H. Arp, G. D. Breedveld, G. A. Slinde, Å. Høiseter, H. M. Grønning, M. Jartun, T. Rundberget, B. M. Jenssen and S. E. Hale, Paper product production identified as the main source of per- and polyfluoroalkyl substances (PFAS) in a Norwegian lake: source and historic emission tracking, *Environ. Pollut.*, 2021, **273**, 116259.

76 J. P. Benskin, V. Phillips, V. L. St. Louis and J. W. Martin, Source Elucidation of Perfluorinated Carboxylic Acids in Remote Alpine Lake Sediment Cores, *Environ. Sci. Technol.*, 2011, **45**, 7188–7194.

77 S. Fang, C. Li, L. Zhu, H. Yin, Y. Yang, Z. Ye and I. T. Cousins, Spatiotemporal distribution and isomer profiles of perfluoroalkyl acids in airborne particulate matter in Chengdu City, China, *Sci. Total Environ.*, 2019, **689**, 1235–1243.

78 J. Wu, H. Jin, L. Li, Z. Zhai, J. W. Martin, J. Hu, L. Peng and P. Wu, Atmospheric perfluoroalkyl acid occurrence and isomer profiles in Beijing, China, *Environ. Pollut.*, 2019, **255**, 113129.

79 B. Place, *Suspect List of Possible Per- And Polyfluoroalkyl Substances (PFAS) Version 1.5.0*, National Institute of Standards and Technology, 2021, DOI: **10.18434/MDS2-2387**.

80 B. Bugsel and C. Zwiener, LC-MS screening of poly- and perfluoroalkyl substances in contaminated soil by Kendrick mass analysis, *Anal. Bioanal. Chem.*, 2020, **412**, 4797–4805.

81 Y. Liu, A. D. S. Pereira and J. W. Martin, Discovery of $C_5$–$C_{17}$ Poly- and Perfluoroalkyl Substances in Water by In-Line SPE-HPLC-Orbitrap with In-Source Fragmentation Flagging, *Anal. Chem.*, 2015, **87**, 4260–4268.

82 R. R. Draxler and G. D. Hess, An overview of the HYSPLIT_4 modeling system of trajectories, dispersion, and deposition, *Aust. Meteor. Mag.*, 1998, **47**, 295–308.

83 A. F. Stein, R. R. Draxler, G. D. Rolph, B. J. B. Stunder, M. D. Cohen and F. Ngan, NOAA's HYSPLIT Atmospheric Transport and Dispersion Modeling System, *Bull. Am. Meteorol. Soc.*, 2015, **96**, 2059–2077.

84 H. Tsugawa, T. Cajka, T. Kind, Y. Ma, B. Higgins, K. Ikeda, M. Kanazawa, J. VanderGheynst, O. Fiehn and M. Arita, MS-DIAL: data-independent MS/MS deconvolution for comprehensive metabolome analysis, *Nat. Methods*, 2015, **12**, 523–526.

85 E. N. Pieke, K. Granby, X. Trier and J. Smedsgaard, A framework to estimate concentrations of potentially unknown substances by semi-quantification in liquid chromatography electrospray ionization mass spectrometry, *Anal. Chim. Acta*, 2017, **975**, 30–41.

86 National Weather Service Forecast Office: Cleveland, OH, *NOWData – NOAA Online Weather Data*, **https://w2.weather.gov/climate/xmacis.php?wfo=cle**, (accessed 13 July 2020).

87 BP4NTA, *NTA Study Reporting Tool (PDF)*, figshare, 2022, DOI: **10.6084/M9.FIGSHARE.19763482**.

88 K. T. Peter, A. L. Phillips, A. M. Knolhoff, P. R. Gardinali, C. A. Manzano, K. E. Miller, M. Pristner, L. Sabourin, M. W. Sumarah, B. Warth and J. R. Sobus, Nontargeted Analysis Study Reporting Tool: A Framework to Improve Research Transparency and Reproducibility, *Anal. Chem.*, 2021, **93**, 13870–13879.

89 R Core Team, *R: A Language and Environment for Statistical Computing*, **https://www.R-project.org/**.

90 E. Kalnay, M. Kanamitsu, R. Kistler, W. Collins, D. Deaven, L. Gandin, M. Iredell, S. Saha, G. White, J. Woollen, Y. Zhu, A. Leetmaa, R. Reynolds, M. Chelliah, W. Ebisuzaki, W. Higgins, J. Janowiak, K. C. Mo, C. Ropelewski, J. Wang, R. Jenne and D. Joseph, The NCEP/NCAR 40-Year Reanalysis Project, *Bull. Am. Meteorol. Soc.*, 1996, **77**, 437–471.

91 J. P. Koelmel, M. K. Paige, J. J. Aristizabal-Henao, N. M. Robey, S. L. Nason, P. J. Stelben, Y. Li, N. M. Kroeger, M. P. Napolitano, T. Savvaides, V. Vasiliou, P. Rostkowski, T. J. Garrett, E. Lin, C. Deigl, K. Jobst, T. G. Townsend, K. J. Godri Pollitt and J. A. Bowden, Toward Comprehensive Per- and Polyfluoroalkyl Substances Annotation Using FluoroMatch Software and Intelligent High-Resolution Tandem Mass Spectrometry Acquisition, *Anal. Chem.*, 2020, **92**, 11186–11194.

92 J. A. Charbonnet, C. A. McDonough, F. Xiao, T. Schwichtenberg, D. Cao, S. Kaserzon, K. V. Thomas, P. Dewapriya, B. J. Place, E. L. Schymanski, J. A. Field, D. E. Helbling and C. P. Higgins, Communicating Confidence of Per- and Polyfluoroalkyl Substance Identification *via* High-Resolution Mass Spectrometry, *Environ. Sci. Technol. Lett.*, 2022, **9**, 473–481.

93 H.-J. Lehmler, Synthesis of environmentally relevant fluorinated surfactants—a review, *Chemosphere*, 2005, **58**, 1471–1496.

94 K. A. Barzen-Hanson, S. C. Roberts, S. Choyke, K. Oetjen, A. McAlees, N. Riddell, R. McCrindle, P. L. Ferguson, C. P. Higgins and J. A. Field, Discovery of 40 Classes of Per- and Polyfluoroalkyl Substances in Historical Aqueous Film-Forming Foams (AFFFs) and AFFF-Impacted Groundwater, *Environ. Sci. Technol.*, 2017, **51**, 2047–2057.

95 R. A. García, A. C. Chiaia-Hernández, P. A. Lara-Martin, M. Loos, J. Hollender, K. Oetjen, C. P. Higgins and J. A. Field, Suspect Screening of Hydrocarbon Surfactants in AFFFs and AFFF-Contaminated Groundwater by High-Resolution Mass Spectrometry, *Environ. Sci. Technol.*, 2019, **53**, 8068–8077.

96 A. Koch, S. Yukioka, S. Tanaka, L. W. Y. Yeung, A. Kärrman and T. Wang, Characterization of an AFFF impacted freshwater environment using total fluorine, extractable organofluorine and suspect per- and polyfluoroalkyl substance screening analysis, *Chemosphere*, 2021, **276**, 130179.

97 K.-U. Goss, The p$K_a$ Values of PFOA and Other Highly Fluorinated Carboxylic Acids, *Environ. Sci. Technol.*, 2008, **42**, 456–458.

98 K. Prevedouros, I. T. Cousins, R. C. Buck and S. H. Korzeniowski, Sources, Fate and Transport of Perfluorocarboxylates, *Environ. Sci. Technol.*, 2006, **40**, 32–44.

99 D. A. Ellis, J. W. Martin, A. O. De Silva, S. A. Mabury, M. D. Hurley, M. P. Sulbaek Andersen and T. J. Wallington, Degradation of Fluorotelomer Alcohols: A Likely Atmospheric Source of Perfluorinated Carboxylic Acids, *Environ. Sci. Technol.*, 2004, **38**, 3316–3321.

100 M. M. Schultz, D. F. Barofsky and J. A. Field, Fluorinated Alkyl Surfactants, *Environ. Eng. Sci.*, 2003, **20**, 487–501.

101 J. P. Benskin, M. Bataineh and J. W. Martin, Simultaneous Characterization of Perfluoroalkyl Carboxylate, Sulfonate, and Sulfonamide Isomers by Liquid Chromatography–Tandem Mass Spectrometry, *Anal. Chem.*, 2007, **79**, 6455–6464.

102 A. Pellizzaro, A. Zaggia, M. Fant, L. Conte and L. Falletti, Identification and quantification of linear and branched isomers of perfluorooctanoic and perfluorooctane sulfonic acids in contaminated groundwater in the veneto region, *J. Chromatogr. A*, 2018, **1533**, 143–154.

103 T. L. Coggan, T. Anumol, J. Pyke, J. Shimeta and B. O. Clarke, A single analytical method for the determination of 53 legacy and emerging per- and polyfluoroalkyl substances (PFAS) in aqueous matrices, *Anal. Bioanal. Chem.*, 2019, **411**, 3507–3520.

104 J. H. Johansson, H. Yan, U. Berger and I. T. Cousins, Water-to-air transfer of branched and linear PFOA: influence of pH, concentration and water type, *Emerging Contam.*, 2017, **3**, 46–53.

105 Y. Wen, Á. Rentería-Gómez, G. S. Day, M. F. Smith, T.-H. Yan, R. O. K. Ozdemir, O. Gutierrez, V. K. Sharma, X. Ma and H.-C. Zhou, Integrated Photocatalytic Reduction and Oxidation of Perfluorooctanoic Acid by Metal–Organic Frameworks: Key Insights into the Degradation Mechanisms, *J. Am. Chem. Soc.*, 2022, **144**, 11840–11850.

106 L. J. Winchell, J. J. Ross, M. J. M. Wells, X. Fonoll, J. W. Norton and K. Y. Bell, Per- and polyfluoroalkyl substances thermal destruction at water resource recovery facilities: a state of the science review, *Water Environ. Res.*, 2021, **93**, 826–843.

 

107 J. Horst, J. McDonough, I. Ross and E. Houtz, Understanding and Managing the Potential By-Products of PFAS Destruction, *Groundwater Monit. Rem.*, 2020, **40**, 17–27.

108 G. K. Longendyke, S. Katel and Y. Wang, PFAS fate and destruction mechanisms during thermal treatment: a comprehensive review, *Environ. Sci.: Processes Impacts*, 2022, **24**, 196–208.

109 M. Altarawneh, M. H. Almatarneh and B. Z. Dlugogorski, Thermal decomposition of perfluorinated carboxylic acids: kinetic model and theoretical requirements for PFAS incineration, *Chemosphere*, 2022, **286**, 131685.

110 F. Xiao, P. C. Sasi, B. Yao, A. Kubátová, S. A. Golovko, M. Y. Golovko and D. Soli, Thermal Stability and Decomposition of Perfluoroalkyl Substances on Spent Granular Activated Carbon, *Environ. Sci. Technol. Lett.*, 2020, **7**, 343–350.

111 U.S. Environmental Protection Agency, Method 533: Determination of Per- and Polyfluoroalkyl Substances in Drinking Water by Isotope Dilution Anion Exchange Solid Phase Extraction and Liquid Chromatography/Tandem Mass Spectrometry, 2019, **https://www.epa.gov/sites/default/files/2019-12/documents/method-533-815b19020**.

112 U.S. Environmental Protection Agency, Method 537.1: Determination of Selected Per- and Polyfluorinated Alkyl Substances in Drinking Water by Solid Phase Extraction and Liquid Chromatography/Tandem Mass Spectrometry (LC/MS/MS), 2018, **https://cfpub.epa.gov/si/si_public_file_download.cfm?p_download_id=537290&Lab=NERL**.

113 Environmental Protection Agency, Lifetime Drinking Water Health Advisories for Four Perfluoroalkyl Substances, *Fed. Regist.*, 2022, **87**, 36848–36849.

114 M. Berg, S. R. Müller, J. Mühlemann, A. Wiedmer and R. P. Schwarzenbach, Concentrations and Mass Fluxes of Chloroacetic Acids and Trifluoroacetic Acid in Rain and Natural Waters in Switzerland, *Environ. Sci. Technol.*, 2000, **34**, 2675–2683.

115 S. Joudan, A. O. De Silva and C. J. Young, Insufficient evidence for the existence of natural trifluoroacetic acid, *Environ. Sci.: Processes Impacts*, 2021, **23**, 1641–1649.

116 M. Scheurer, K. Nödler, F. Freeling, J. Janda, O. Happel, M. Riegel, U. Müller, F. R. Storck, M. Fleig, F. T. Lange, A. Brunsch and H.-J. Brauch, Small, mobile, persistent: trifluoroacetate in the water cycle – overlooked sources, pathways, and consequences for drinking water supply, *Water Res.*, 2017, **126**, 460–471.

117 M. Ateia, A. Maroli, N. Tharayil and T. Karanfil, The overlooked short- and ultrashort-chain poly- and perfluorinated substances: a review, *Chemosphere*, 2019, **220**, 866–882.

118 R. W. Helmer, D. M. Reeves and D. P. Cassidy, Per- and Polyfluorinated Alkyl Substances (PFAS) cycling within Michigan: Contaminated sites, landfills and wastewater treatment plants, *Water Res.*, 2022, **210**, 117983.